Ionic Metallomesogens. Lamellar Mesophases in Copper(I) Azamacrocyclic Complexes

Francesco Neve* and Mauro Ghedini

Dipartimento di Chimica, Università della Calabria, I-87030 Arcavacata di Rende (CS), Italy

Anne-Marie Levelut

Laboratoire de Physique des Solides, associé au CNRS, Université Paris-Sud, F-91405 Orsay Cedex, France

Oriano Francescangeli

Dipartimento di Scienze dei Materiali e della Terra, Sezione Fisica, Università di Ancona, Via Breccie Bianche, I-60131 Ancona, Italy

Received August 2, 1993. Revised Manuscript Received October 26, 1993®

A series of nonmesogenic N-acylated derivatives (**2**) of 1,10-diaza-4,7,13,16-tetrathiacyclooctadecane (**1**) affords stable cationic complexes upon reaction with $[Cu(MeCN)_4][PF_6]$. The products $[Cu(\mathbf{2})][PF_6]$ show thermotropic mesomorphism as a result of copper(I) complexation. Optical microscopy, calorimetry, and low-resolution powder X-ray diffraction were used to characterize the liquid-crystalline order. The presence in all complexes of a single mesophase with a lamellar structure is proposed and discussed.

Introduction

Macrocyclic metallomesogens represent an important family of thermotropic mesogens, whose interesting properties are mainly due to the presence of metal ions (either main-group or transition metals) in the central organic core.[1,2] The vast majority are metallic complexes containing phthalocyanines[3–6] or porphyrines[7–9] as ligands. Mesogenic metal derivatives of porphyrazines[10,11] and dibenzotetraaza[14]annulenes[12] have also been described.

Macrocyclic metallomesogens usually consist of disk-shaped units (bearing several hydrocarbon tails) which assemble into columns. Columnar-discotic mesophases are therefore characteristic of this class of mesogens.[13]

A very few examples of metallomesogens with *saturated* macrocyclic ligands are currently known. These are ionic complexes of substituted polyaza coronands. So far, mesogenic Co(III), Ni(II), or Cu(II) adducts with amine derivatives of 1,4,7,10,13,16-hexaazacyclooctadecane,[14] 1,4,8,11-tetraazacyclotetradecane,[14] and 1,4,7-triazacyclononane[15] have been reported. Mesophase structures have been described as columnar with various degree of disorder. A disordered zig-zag lamello-columnar structure was suggested for the mesomorphic state of a triazacyclononane Ni(II) complex.[15]

Most metallomesogens are molecular materials. Besides the ionic amphiphilic metal soaps,[1a] *thermotropic ionic metallomesogens*[16–20] are mainly represented by linear silver(I) pyridine complexes.[16,17] Although some of them show thermal instability in the isotropic state or decompose in the mesophase under X-ray irradiation, all ionic silver

® Abstract published in *Advance ACS Abstracts,* December 1, 1993.

(1) (a) Giroud-Godquin, A. M.; Maitlis, P. M. *Angew. Chem., Int. Ed. Engl.* **1991**, *30*, 375. (b) Espinet, P.; Esteruelas, M. A.; Oro, L. A.; Serrano, J. L.; Sola, E. *Coord. Chem. Rev.* **1992**, *117*, 215. (c) Hudson, S. A.; Maitlis, P. M. *Chem. Rev.* **1993**, *93*, 861.

(2) Bruce, D. W. In *Inorganic Materials*; Bruce, D. W., O'Hare, D., Eds.; Wiley: Chichester, UK, 1992; pp 405–490.

(3) (a) Piechocki, C.; Simon, J.; Skoulios, A.; Guillon, D.; Weber, P. *J. Am. Chem. Soc.* **1982**, *104*, 5245. (b) Guillon, D.; Weber, P.; Skoulios, A.; Piechocki, C.; Simon, J. *Mol. Cryst. Liq. Cryst.* **1985**, *130*, 223. (c) Piechocki, C.; Simon, J.; André, J.-J.; Guillon, D.; Petit, P.; Skoulios, A.; Weber, P. *Chem. Phys. Lett.* **1985**, *122*, 124. (d) Sirlin, C.; Bosio, L.; Simon, J. *J. Chem. Soc., Chem. Commun.* **1987**, 379; **1988**, 236; *Mol. Cryst. Liq. Cryst.* **1988**, *155*, 231. (e) Piechocki, C.; Boulou, J. C.; Simon, J. *Mol. Cryst. Liq. Cryst.* **1987**, *149*, 115. (f) Simon, J.; Sirlin, C. *Pure Appl. Chem.* **1989**, *61*, 1625. (g) Belarbi, Z.; Sirlin, C.; Simon, J.; André, J.-J. *J. Phys. Chem.* **1989**, *93*, 8105.

(4) Cook, M. J.; Daniel, M. F.; Harrison, K. J.; McKeown, N. B.; Thomson, A. *J. Chem. Soc., Chem. Commun.* **1987**, 1086.

(5) Hanack, M.; Beck, A.; Lehmann, H. *Synthesis* **1987**, 703.

(6) van der Pol, J. F.; Neeleman, E.; Zwikker, J. W.; Nolte, R. J. M.; Drenth, W.; Aerts, J.; Wisser, R.; Picken, S. J. *Liq. Cryst.* **1989**, *6*, 577.

(7) Gregg, B. A.; Fox, M. A.; Bard, A. J. *J. Am. Chem. Soc.* **1989**, *111*, 3024.

(8) Kugimiya, S.; Takemura, M. *Tetrahedron Lett.* **1990**, *31*, 3157.

(9) Shimizu, Y.; Miya, M.; Nagata, A.; Ohta, K.; Matsumara, A.; Yamamoto, I.; Kusubayashi, S. *Chem. Lett.* **1991**, 25.

(10) Doppelt, P.; Huille, S. *New J. Chem.* **1990**, *14*, 607.

(11) Ohta, K.; Watanabe, T.; Fujimoto, T.; Yamamoto, I. *J. Chem. Soc., Chem. Commun.* **1989**, 1611.

(12) Hunziker, M. EP-B 0162804; *Chem. Abstr.* **1987**, *106*, 41716.

(13) For the only example of *calamitic metalloporphyrines* see: Bruce, D. W.; Dunmur, D. A.; Santa, L. S.; Wali, M. A. *J. Mater. Chem.* **1992**, *2*, 363.

(14) Liebmann, A.; Mertesdorf, C.; Plesnivy, T.; Ringsdorf, H.; Wendorff, J. H. *Angew. Chem., Int. Ed. Engl.* **1991**, *30*, 1375.

(15) Lattermann, G.; Schmidt, S.; Kleppinger, R.; Wendorff, J. H. *Adv. Mater.* **1992**, *4*, 30.

(16) (a) Bruce, D. W.; Dunmur, D. A.; Lalinde, E.; Maitlis, P. M.; Styring, P. *Nature* **1986**, *323*, 791. (b) Bruce, D. W.; Dunmur, D. A.; Maitlis, P. M.; Styring, P.; Esteruelas, M. A.; Oro, L. A.; Ros, M. B.; Serrano, J. L.; Sola, E. *Chem. Mater.* **1989**, *1*, 479. (c) Bruce, D. W.; Dunmur, D. A.; Hudson, S. A.; Lalinde, E.; Maitlis, P. M.; McDonald, M. P.; Orr, R.; Styring, P.; Cherodian, A. S.; Richardson, R. M.; Feijoo, J. L.; Ungar, G. *Mol. Cryst. Liq. Cryst.* **1991**, *206*, 79. (d) Adams, H.; Bailey, N. A.; Bruce, D. W.; Davis, S. C.; Dunmur, D. A.; Hempstead, P. D.; Hudson, S. A.; Thorpe, S. *J. Mater. Chem.* **1992**, *2*, 395. (e) Bruce, D. W.; Davis, S. C.; Dunmur, D. A.; Hudson, S. A.; Maitlis, P. M.; Styring, P. *Mol. Cryst. Liq. Cryst. Sci. Technol., Sect. A* **1992**, *215*, 1; *Adv. Mater. Opt. Electron.* **1992**, *1*, 37.

(17) Marcos, M.; Ros, M. B.; Serrano, J. L.; Esteruelas, M. A.; Sola, E.; Oro, L. A.; Barbera, J. *Chem. Mater.* **1990**, *2*, 748.

(18) Paleos, G. M.; Margomenou-Lenidopoulou, G.; Anastassopoulou, J. D.; Papaconstantinou, E. *Mol. Cryst. Liq. Cryst.* **1988**, *161*, 373.

(19) (a) Markovitsi, D.; Bernard, M.; André, J.-J.; Simon, J. *J. Phys. Chem.* **1986**, *90*, 1323. (b) Markovitsi, D.; André, J.-J.; Mathis, A.; Simon, J.; Spegt, P.; Weill, G.; Ziliox, M. *Chem. Phys. Lett.* **1984**, *104*, 46.

(20) Ghedini, M.; Pucci, D. *J. Organomet. Chem.* **1990**, *395*, 105.

0897-4756/94/2806-0070$04.50/0

mesogens exhibit pronounced polymorphism which strongly depends on the counteranion nature.

We now report on a series of cationic macrocyclic Cu(I) complexes based on *nonmesogenic* bis[4-(*n*-alkyloxy)benzamide] derivatives (**2**) of 1,10-diaza-4,7,13,16-tetrathiacyclooctadecane (**1**). Thermotropic mesomorphism was previously observed for the cationic species $[Pd(L)][Y]_2$ (L = 1,10-bis[4-(dodecyloxy)benzoyl]-1,10-diaza-4,7,13,-16-tetrathiacyclooctadecane (ligand **2d**) and $Y = BF_4^-$), whose mesophase structure was not conclusively assigned.[21]

Experimental Section

Reagents. Anhydrous *N,N*-dimethylacetamide (Aldrich), 4-(dimethylamino)pyridine (Aldrich), and 1,10-diaza-4,7,13,16-tetrathiacyclooctadecane (Lancaster) were used as received. 4-(*n*-Alkyloxy)benzoyl chlorides[22] and $[Cu(MeCN)_4][PF_6]$[23] were synthesized according to the literature.

General Methods. Unless otherwise stated all reactions were performed under a dry argon atmosphere in freshly distilled solvents.

^1H and ^{13}C NMR spectra were recorded on a Bruker WH 300 spectrometer with internal tetramethylsilane as reference. Infrared spectra were recorded on a Perkin-Elmer System-2000 FT-IR spectrometer. Conductivity measurements were carried out using an LKB 5300 B Conductolyser conductivity bridge. Mass spectra were recorded by fast-atom bombardment on a VG-ZAB mass spectrometer. Elemental analyses were performed at the Microanalytical Laboratory of our department.

Optical observations were carried out with a Zeiss Axioskop polarizing microscope equipped with a Linkam CO 600 heating stage and temperature control. Transition temperatures were measured by differential scanning calorimetry (DSC) with a Perkin-Elmer DSC-7 instrument operating at a scanning rate of 10 °C/min.

X-ray diffraction measurements on powder samples were performed with an INEL CPS 120 powder diffractometer equipped with a position-sensitive detector covering 120° in the scattering angle 2θ, with an angular resolution of 0.018°. Monochromatized Cu Kα (λ = 1.54 Å) radiation was used. The samples, ≈1 mm thick, were placed between two thin Al sheets, fixed to a circular hole (1-cm diameter) in an Al sample holder. Heating was achieved by a hot stage with control stability ±0.1 °C.

(a) Syntheses of Ligands. The preparation of ligands **2a** and **2d** (*n*-hexyloxy and *n*-dodecyloxy homologues, respectively) has been previously reported.[21] Ligands **2b**, **2c**, and **2e** have been prepared following the same procedure with different reflux time. They were all obtained as white solids by crystallization of a crude yellow oil in *n*-hexane at −20 °C.

1,10-Bis[4-(decyloxy)benzoyl]-1,10-diaza-4,7,13,16-tetrathiacyclooctadecane (2b). Reflux time 48 h. Yield 63%. Mp (DSC) 74 °C. Anal. Calcd for $C_{46}H_{74}N_2O_4S_4$: C, 65.24; H, 8.80; N, 3.31. Found: C, 65.15; H, 8.83; N, 3.19. IR (neat) 2925 (s), 2856 (m), 1632 (vs), 1610 (s), 1513 (m), 1465 (s), 1423 (s), 1297 (s), 1251 (vs), 1240 (s), 1175 (s), 1128 (s), 1019 (s), 843 (s) cm^{-1}. ^1H NMR (300 MHz, C_6D_6, 298 K) δ 0.96 (t, 3 H, CH_3), 1.31 (m, 14 H, $(CH_2)_7$), 1.64 (m, 2 H, O–CH_2–CH_2), 2.66 (v br s, 8 H, CH_2–S–CH_2), 3.58 (v br s, 4 H, N–CH_2), 3.63 (t, 2 H, O–CH_2), 6.84 (d, 2 H, arom 3, 5), 7.50 (d, 2 H, arom 2, 6). $^{13}C\{^1H\}$ NMR (75.47, C_6D_6, 298 K) δ 14.97, 23.73, 27.08, 30.24, 30.40, 30.43, 30.64, 31.92 (br), 32.96, 33.90 (br), 49.85 (v br), 68.85, 115.26, 129.91, 130.09, 161.42, 172.42.

1,10-Bis[4-(undecyloxy)benzoyl]-1,10-diaza-4,7,13,16-tetrathiacyclooctadecane (2c). Reflux time 40 h. Yield 69%. Mp (DSC) 75 °C. Anal. Calcd for $C_{48}H_{78}N_2O_4S_4$: C, 65.86; H, 8.98; N, 3.20. Found: C, 66.03; H, 9.08; N, 3.09. IR (Nujol) 1627 (s), 1609 (m), 1512 (m), 1464 (br s), 1295 (m), 1250 (s), 1176 (m), 1127 (m), 841 (s) cm^{-1}. ^1H NMR (300 MHz, C_6D_6, 298 K) δ 0.96 (t, 3 H, CH_3), 1.33 (m, 16 H, $(CH_2)_8$), 1.65 (m, 2 H, O–CH_2–CH_2), 2.64 (br s, 8 H, CH_2–S–CH_2), 3.56 (br s, 4 H, N–CH_2), 3.63 (t, 2 H, O–CH_2), 6.83 (d, 2 H, arom 3, 5), 7.49 (d, 2 H, arom 2, 6). $^{13}C\{^1H\}$ NMR (75.47, C_6D_6, 298 K) δ 14.97, 23.74, 27.08, 30.24, 30.44, 30.66, 30.70, 31.90 (br), 32.97, 33.87 (br), 49.86 (br), 68.83, 115.24, 129.94, 130.08, 161.41, 172.35.

1,10-Bis[4-(tetradecyloxy)benzoyl]-1,10-diaza-4,7,13,16-tetrathiacyclooctane (2e). Reflux time 22 h. Yield 67%. Mp (DSC) 76 °C (first heating), 74 °C (second and further heatings). Anal. Calcd for $C_{54}H_{90}N_2O_4S_4$: C, 67.59; H, 9.45; N, 2.92. Found: C, 67.82; H, 9.47; N, 2.88. IR (Nujol) 1630 (vs), 1609 (m), 1511 (m), 1467 (br s), 1409 (m), 1302 (s), 1252 (s), 1238 (s), 1172 (s), 1147 (m), 1135 (m), 1011 (m), 841 (s) cm^{-1}. ^1H NMR (300 MHz, C_6D_6, 298 K) δ 0.96 (t, 3 H, CH_3), 1.36 (br s, 22 H, $(CH_2)_{11}$), 1.66 (m, 2 H, O–CH_2–CH_2), 2.65 (br s, 8 H, CH_2–S–CH_2), 3.58 (br s, 4 H, N–CH_2), 3.65 (t, 2 H, O–CH_2), 6.83 (d, 2 H, arom 3, 5), 7.49 (d, 2 H, arom 2, 6). $^{13}C\{^1H\}$ NMR (75.47, C_6D_6, 298 K) δ 14.87, 23.69, 27.10, 30.29, 30.40, 30.44, 30.65, 30.68, 30.73, 30.77, 32.11 (br), 32.96, 34.06 (br), 49.92 (v br), 69.00, 115.38, 130.04, 130.14, 161.49, 172.27.

(b) Synthesis of the Complexes. A typical procedure is reported for the preparation of [Cu(**2d**)][PF_6].

A solution of **2d** (106 mg, 0.117 mol) in CH_2Cl_2 (4 mL) was added to a stirred solution of an equimolar amount of $[Cu(CH_3CN)_4][PF_6]$ in CH_3CN (5 mL). Stirring was continued for 1 h, whereupon the solvents were evaporated to a small volume (ca. 1 mL), and diethyl ether was added to give a white precipitate. The solid was filtered off and redissolved in the minimum amount of CH_2Cl_2, and the solution evaporated to dryness. The product was recovered as a white microcrystalline solid in 84% yield (110 mg). FAB mass spectrum (3-nitrobenzyl alcohol matrix) *m/z* 965 ($[^{63}Cu(\mathbf{2d})]^+$). Anal. Calcd for $C_{50}H_{82}F_6N_2O_4PS_4Cu$: C, 54.01; H, 7.43; N, 2.52. Found: C, 53.10; H, 7.25; N, 2.57. IR (Nujol) ν(C=O) 1635 (s), ν(PF) 840 (s br) cm^{-1}. Λ_M (1×10^{-4} M in nitromethane solution) 76.07 Ω^{-1} mol^{-1} cm^2. ^1H NMR (300 MHz, CD_3NO_2–CD_3CN, 298 K) δ 0.88 (t, 3 H, CH_3), 1.29–1.47 (m, 18 H, $(CH_2)_9$), 1.79 (m, 2 H, O–CH_2–CH_2), 2.97 (br s, 8 H, CH_2–S–CH_2), 3.65 (br t, 4 H, N–CH_2), 4.03 (t, 2 H, O–CH_2), 6.99 (d, 2 H, arom 3, 5), 7.49 (d, 2 H, arom 2, 6). $^{13}C\{^1H\}$ NMR (75.47, CD_3NO_2–CD_3CN, 298 K) δ 13.66, 22.74, 26.15, 29.35, 29.43, 29.48, 29.70, 29.74, 29.76, 32.03, 33.86 (S–CH_2–CH_2–N), 35.00 (S–CH_2–CH_2–S), 47.90 (N–CH_2), 68.67 (OCH_2), 114.74, 128.79, 129.47, 160.93, 173.59.

[Cu(2a)]PF_6. Yield 88%. FAB mass spectrum (3-nitrobenzyl alcohol matrix) *m/z* 797 ($[^{63}Cu(\mathbf{2a})]^+$). Anal. Calcd for $C_{38}H_{58}F_6N_2O_4PS_4Cu$: C, 48.44; H, 6.20; N, 2.97. Found: C, 47.70; H, 6.10; N, 2.75. IR (Nujol) ν(C=O) 1636 (s), ν(PF) 840 (s br) cm^{-1}. Λ_M (1×10^{-4} M in nitromethane solution) 82.52 Ω^{-1} mol^{-1} cm^2. ^1H NMR (300 MHz, CD_3NO_2–CD_3CN, 298 K) δ 0.91 (t, 3 H, CH_3), 1.32–1.48 (m, 6 H, $(CH_2)_3$), 1.77 (m, 2 H, O–CH_2–CH_2), 2.94 (br s, 4 H, S–CH_2–CH_2–S), 2.96 (t, 4 H, S–CH_2–CH_2–N), 3.63 (t, 4 H, N–CH_2), 4.02 (t, 2 H, O–CH_2), 6.98 (d, 2 H, arom 3, 5), 7.47 (d, 2 H, arom 2, 6). $^{13}C\{^1H\}$ NMR (75.47, CD_3NO_2–CD_3CN, 298 K) 13.47, 22.51, 25.62, 29.12, 31.52, 33.46 (S–CH_2–CH_2–N), 34.67 (S–CH_2–CH_2–S), 47.60 (N–CH_2), 68.47 (OCH_2), 114.56, 128.67, 129.26, 160.09, 173.22.

[Cu(2b)]PF_6. Yield 70%. FAB mass spectrum (3-nitrobenzyl alcohol matrix) *m/z* 909 ($[^{63}Cu(\mathbf{2b})]^+$). Anal. Calcd for $C_{46}H_{74}F_6N_2O_4PS_4Cu$: C, 52.35; H, 7.07; N, 2.66. Found: C, 52.42; H, 7.10; N, 2.82. IR (Nujol): ν(C=O) 1635 (s), ν(PF) 840 (s br) cm^{-1}. Λ_M (1×10^{-4} M in nitromethane solution) 85.26 Ω^{-1} mol^{-1} cm^2. ^1H NMR (300 MHz, CD_3NO_2–CD_3CN, 298 K) δ 0.87 (t, 3 H, CH_3), 1.29–1.47 (m, 14 H, $(CH_2)_7$), 1.79 (m, 2 H, O–CH_2–CH_2), 3.01 (br s, 8 H, CH_2–S–CH_2), 3.67 (br s, 4 H, N–CH_2), 4.03 (t, 2 H, O–CH_2), 7.00 (d, 2 H, arom 3, 5), 7.52 (d, 2 H, arom 2, 6). $^{13}C\{^1H\}$ NMR (75.47, CD_3NO_2–CD_3CN, 298 K) 13.45, 22.57, 25.97, 29.16, 29.24, 29.32, 29.50, 29.53, 31.85, 33.99 (S–CH_2–CH_2–N), 35.00 (S–CH_2–CH_2–S), 47.57 (N–CH_2), 68.45 (OCH_2), 114.48, 128.43, 129.33, 160.78, 173.66.

[Cu(2c)]PF_6. Yield 69%. FAB mass spectrum (3-nitrobenzyl alcohol matrix) *m/z* 937 ($[^{63}Cu(\mathbf{2c})]^+$). Anal. Calcd for $C_{48}H_{78}F_6N_2O_4PS_4Cu$: C, 53.22; H, 7.26; N, 2.59. Found: C, 53.10; H, 7.28; N, 2.74. IR (Nujol) ν(C=O) 1631 (s), ν(PF) 841 (s br) cm^{-1}. Λ_M (1×10^{-4} M in nitromethane solution) 80.66 Ω^{-1} mol^{-1} cm^2. ^1H NMR (300 MHz, CD_3NO_2, 298 K) δ 0.86 (t, 3 H, CH_3), 1.29–1.47 (m, 16 H, $(CH_2)_8$), 1.80 (m, 2 H, O–CH_2–CH_2), 3.05 (br

(21) Neve, F.; Ghedini, M. *J. Inclusion Phenom.* **1993**, *15*, 259.
(22) Tatarsky, D.; Banerjee, K.; Ford, W. T. *Chem. Mater.* **1990**, *2*, 138.
(23) Kubas, G. J. *Inorg. Synth.* **1979**, *19*, 90.

Scheme I

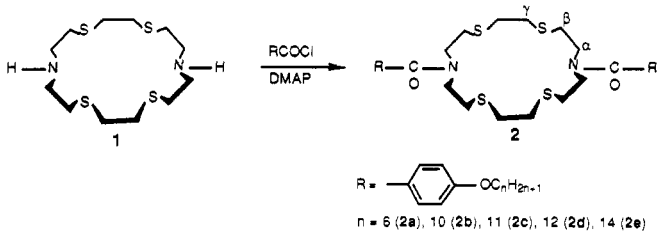

s, 8 H, CH_2-S-CH_2), 3.70 (br s, 4 H, N-CH_2), 4.04 (t, 2 H, O-CH_2), 7.01 (d, 2 H, arom 3, 5), 7.55 (d, 2 H, arom 2, 6). $^{13}C\{^1H\}$ NMR (75.47, CD_3NO_2, 298 K) 13.52, 22.73, 26.15, 29.34, 29.43, 29.51, 29.72, 32.03, 34.37 (S-CH_2-CH_2-N), 35.29 (S-CH_2-CH_2-S), 47.67 (N-CH_2), 68.66 (OCH_2), 114.66, 128.60, 129.56, 161.03, 174.06.

[Cu(2e)]PF_6. Yield 65%. FAB mass spectrum (3-nitrobenzyl alcohol matrix) m/z 1021 ($[^{63}Cu(\mathbf{2e})]^+$). Anal. Calcd for $C_{54}H_{90}F_6N_2O_4PS_4Cu$: C, 55.53; H, 7.77; N, 2.40. Found: C, 54.70; H, 7.58; N, 2.60. IR (Nujol) ν(C=O) 1635 (s), ν(PF) 840 (s br) cm^{-1}. Λ_M (1×10^{-4} M in nitromethane solution) 86.77 Ω^{-1} mol^{-1} cm^2. ^1H NMR (300 MHz, CD_3NO_2, 298 K) δ 0.85 (t, 3 H, CH_3), 1.28-1.47 (m, 22 H, $(CH_2)_{11}$), 1.80 (m, 2 H, O-CH_2-CH_2), 3.04 (br s, 8 H, CH_2-S-CH_2), 3.78 (br s, 4 H, N-CH_2), 4.03 (t, 2 H, O-CH_2), 7.01 (d, 2 H, arom 3, 5), 7.55 (d, 2 H, arom 2, 6). $^{13}C\{^1H\}$ NMR (75.47, CD_3NO_2, 298 K) 13.49, 22.71, 26.15, 29.34, 29.42, 29.51, 29.72, 29.76, 32.02, 34.37 (S-CH_2-CH_2-N), 35.29 (S-CH_2-CH_2-S), 47.65 (N-CH_2), 68.66 (OCH_2), 114.65, 128.58, 129.55, 161.03, 174.10.

Results and Discussion

Solution Studies. The cyclic diazatetrathia ether 1 was acylated by a series of acyl chlorides in a manner similar to that reported by Lehn[24] or Heiney[25] and coworkers (Scheme 1).

The bis(amide) derivatives **2** are obtained in fairly good yields as white air-stable solids. The synthesis of **2a** and **2d** has been previously reported.[21]

Compounds **2** have relatively simple ^1H NMR spectra which can be divided in three different regions. Two of them (at 7.60-6.80 and 1.80-0.80 ppm, respectively) involve well-resolved signals which arise from the aromatic and aliphatic protons of the appended tails. The third region (4.1-2.7 ppm), apart from a triplet due to the OCH_2 protons, shows the methylene resonances for the central, hollow portion of the ligands. These appear as broad signals probably due to conformational fluxionality of the core. The $^{13}C\{^1H\}$ NMR spectra of **2** are regular except for the very broad resonance at δ ca. 50 ppm assigned to the α carbons.

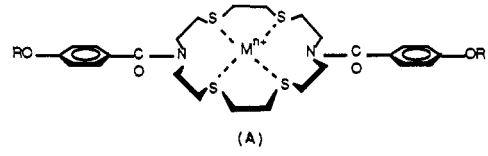

(A)

In principle, the N_2S_4 donor set of **2** could afford hexacoordinated complexes upon coordination of metal ions. However, given the low donor ability of amide nitrogens tetracoordination through S donors (structure **A**) is much more likely. The macrocyclic cavity of **2** has such geometrical features as either a square-planar or a tetrahedral coordination geometry can be accommodated. While the former geometry is believed to occur in [Pd(L)][BF_4]$_2$ (L = **2a**, **2d**),[21] the latter has been crystallographically established for [Cu(L)][PF_6] (L = 1,10-bis(ferrocenemethyl)-1,10-diaza-4,7,13,16-tetrathiacyclooctadecane).[26a] The solid-state structure of the complex, which contains a ligand with a donor environment very similar to that of **2**, shows a Cu(I) ion bound to a distorted-tetrahedral array of S donors. The only other example of Cu(I) coordination to an 18-membered N_2S_4 macrocycle refers to the binuclear [$Cu_2(Me_2[18]aneN_2S_4)$-$(MeCN)_2$]$^+$, wherein each Cu(I) center is bound tetrahedrally to one N and two S donors of the macrocycle.[26b,c]

[$Cu(MeCN)_4$][PF_6][23] smoothly reacts with ligands **2** (molar ratio 1:1) in dichloromethane-acetonitrile affording colorless solutions. Dry solvents and an inert atmosphere were used to minimize water presence and copper oxidation. The products are recovered as white, nonhygroscopic, air-stable solids which behave as 1:1 electrolites in nitromethane solutions. The FAB mass spectra of the complexes show a characteristic molecular ion peak with the correct isotopic distribution corresponding to $[^{63}Cu(\mathbf{2})]^+$. This evidence, together with the analytical and IR data, supports the formulation [Cu(**2**)][PF_6].

The ^1H NMR spectra of the cationic [Cu(**2**)][PF_6] show a marked solvent dependence. For example, when the solvent is CD_3NO_2 the proton signals for the saturated ring are very broad. Addition of small amounts of CD_3CN (which also improves the general solubility of the complexes) causes a sharpening of the signals, and multiplicity can be sometimes observed. We believe that either the solvent is not involved in metal coordination or the process is fast on the NMR time scale. On the other hand, the addition of acetonitrile to nitromethane solutions of [Cu(**2**)][PF_6] has a negligible effect on their $^{13}C\{^1H\}$ NMR spectra. These are characterized by sharp signals even for the macrocyclic methylene carbons. In particular, three distinct resonances assigned to those carbon atoms are observed in the range δ 50-33 ppm. A 2-D ^1H-^{13}C correlation experiment for $[Cu(\mathbf{2a})]^+$ in CD_3NO_2-CD_3CN allowed the carbon spectrum to be assigned. The resonance at δ 47.60 (which is related to a triplet at δ 2.96 in the proton spectrum) is assigned to the α carbons. The resonances seen at δ 33.46 and 34.67 (related to a singlet at δ 2.94 and to a broad triplet at δ 2.96, respectively) can be assigned to the γ and β carbon atoms, respectively.

Mesomorphic Behavior. Macrocycles **2**, irrespective of the length of the n-alkoxy chains, melt in a very short temperature range (72-76 °C) showing no mesomorphic properties. The thermal behavior of complexes [Cu(**2**)]-[PF_6] was studied by differential scanning calorimetry (DSC) and polarizing optical microscopy. The results are listed in Table 1.

Although the overall behavior is dominated by decomposition around the clearing point, in all cases but for [Cu(**2a**)][PF_6] (and partially for [Cu(**2e**)][PF_6]) the amount of decomposition can be controlled if during experiments the samples are maintained in the isotropic state for very short periods and if temperatures do not exceed the clearing point by more than 5-10 °C.

All complexes show a similar (and rather anomalous) mesomorphic behavior. On heating a pristine sample the

(24) Lehn, J. M.; Malthête, J.; Levelut, A. M. *J. Chem. Soc., Chem. Commun.* **1985**, 1794.

(25) Idziak, S. H. J.; Maliszewskyj, N. C.; Heiney, P. A.; McCauley, J. P., Jr.; Sprengler, P. A.; Smith, A. B., III *J. Am. Chem. Soc.* **1991**, *113*, 7666.

(26) (a) Beer, P. D.; Nation, J. E.; McWhinnie, S. L. W.; Harman, M. E.; Hursthouse, M. B.; Ogden, M. I.; White, A. H. *J. Chem. Soc., Dalton Trans.* **1991**, 2485. (b) Atkinson, N.; Blake, A. J.; Drew, M. G. B.; Forsyth, G.; Lavery, A. J.; Reid, G.; Schröder, M. *J. Chem. Soc., Chem. Commun.* **1989**, 984. (c) Reid, G.; Schröder, M. *Chem. Soc. Rev.* **1990**, *19*, 239.

Table 1. Phase Behavior for Compounds [Cu(2a–e)][PF_6]

compound	transition[a]	temp,[b] °C	ΔH,[b] kJ/mol
[Cu(**2a**)][PF_6]	C-M	93	4.8
	M-I	198(dec)	
[Cu(**2b**)][PF_6]	C-M	≈96[c]	d
	M-I	139	1.4
	I-M	131	−0.6
[Cu(**2c**)][PF_6]	C-M	≈99[c]	d
	M-I	160	1.6
	I-M	156	−1.1
[Cu(**2d**)][PF_6]	C-M	123	5.1
	M-I	190	1.8
	I-M	180	−1.7
[Cu(**2e**)][PF_6]	C-M	≈101[c]	d
	M-I	211[e]	1.7

[a] C, crystal; M, mesophase; I, isotropic liquid. [b] Data from first DSC cycle. [c] Approximate value (±5). [d] Enthalpy change cannot be measured. [e] Clears with some decomposition.

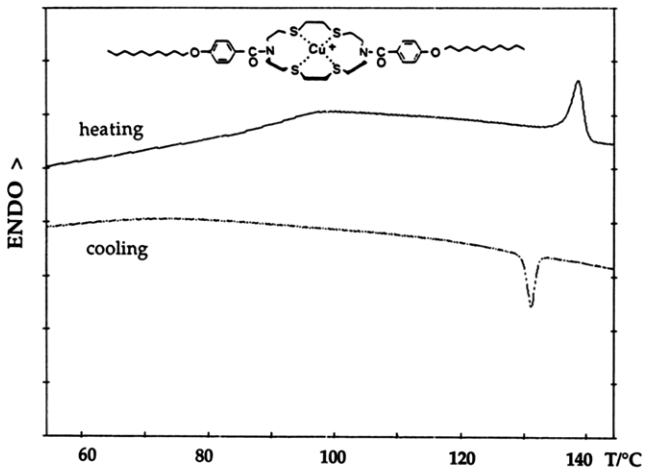

Figure 1. DSC thermogram for [Cu(**2b**)][PF_6] (first cycle).

DSC thermogram exhibits a broad melting transition only in the case of [Cu(**2a**)][PF_6] and [Cu(**2d**)][PF_6]. In the remaining cases, the transition is very slow and the corresponding wide DSC peak usually spans several tens of degrees (Figure 1a). On the other hand, clearing point transitions give rise to rather sharp DSC peaks with small enthalpy values (ΔH = 1.4–2.0 kJ mol^{-1}). On cooling, only the isotropic–anisotropic transition can be seen (Figure 1b). The recrystallization process therefore does not take place, and subsequent heating cycles do not show the melting transition (Figure 2). A decrease in the clearing temperature (2–3 °C) for [Cu(**2b–d**)][PF_6] was observed on second and third heating, which can be ascribed to slight decomposition.

Optical observations confirmed the presence of a single mesophase for all complexes. When a pristine sample is heated, a highly viscous, birefringent phase is obtained at temperatures similar to those observed in DSC experiments under equivalent conditions. The phase viscosity is very high for the lower homologues [Cu(**2a–c**)][PF_6] and decreases with increasing temperature. The texture of the mesophase is better seen on cooling from the melt and is especially clear for [Cu(**2d**)][PF_6] (Figure 3). The occurrence of bâtonnets in the neighborhood of the M–I transition suggests that the mesophase is a smectic phase. Mechanical shearing at temperatures close to the transition induces a considerable deformation of the texture. Optical microscopy also revealed that cooling down to room temperature always affords a frozen mesomorphic texture. Supercooled mesophases have been previously reported for mesogenic Cu[27] and Pd[28] complexes.

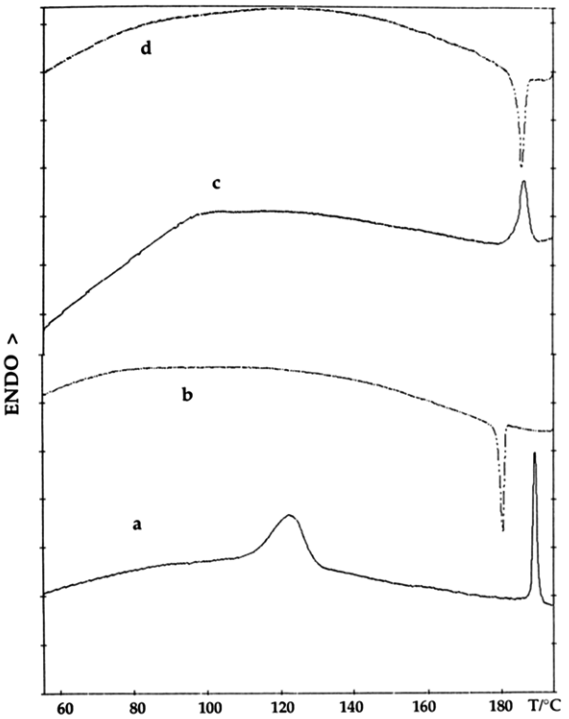

Figure 2. DSC thermograms for [Cu(**2d**)][PF_6]: (a) first heating; (b) first cooling; (c) second heating after a 24 h wait; (d) second cooling.

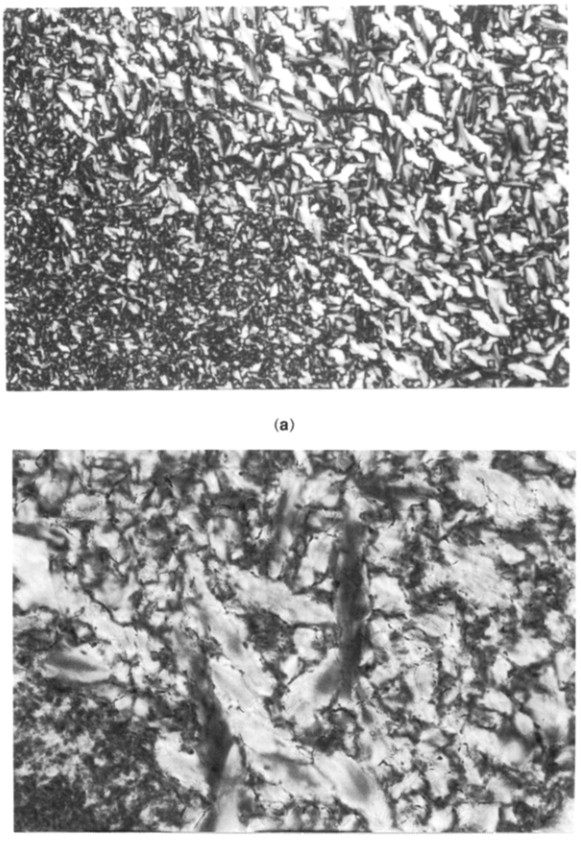

Figure 3. Textures of the mesophase of [Cu(**2d**)][PF_6] between crossed polarizers: (a) on cooling from the isotropic melt to 180 °C (200×); (b) after annealing for 20 min at 175 °C (400×).

Mesophase Structure. Since complex [Cu(**2d**)][PF_6] is the member of the series showing the most clear mesomorphism and sufficient thermal stability, X-ray studies were mainly focused on it.

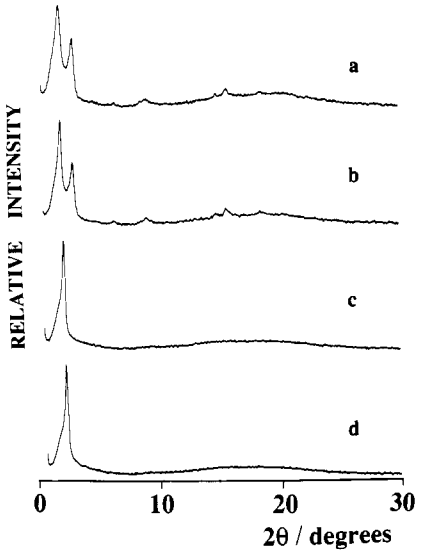

Figure 4. X-ray diffraction spectra of [Cu(**2d**)][PF_6] recorded at different temperatures during a heating cycle: (a) 30; (b) 110; (c) 130; (d) 160 °C.

The room-temperature (RT) X-ray powder diffraction pattern of an unoriented sample of complex [Cu(**2d**)][PF_6] consists of two sharp intense Bragg peaks in the low-angle region and several weak peaks in the higher region, some of which with a diffuse character (Figure 4). The periodicities corresponding to the RT low-angle Bragg peaks are 38.1 and 25.8 Å, while the high-angle reflections are centered at 13 (the second harmonic of the Bragg reflections at 26 Å), 9, 5.9, and 5.6 Å. The latter are superimposed on a broad diffuse halo centered at around 4.7 Å. A further very weak signal at 4.5 Å, which becomes more definite at higher temperatures, can be identified in the RT spectrum. The above X-ray diffraction pattern does not change with temperature until the melting temperature is reached; the only significant variation observed is a shift of the dominant reflection toward lower values of the scattering angle up to 70 °C and, beyond that temperature, toward higher scattering angles. The diffuse character of the high-angle diffraction reflections and the presence of the broad, diffuse halo indicate the partially amorphous nature of the solid phase which is stable up to the melting temperature.

Above the melting point, the X-ray diffraction pattern is featured by one sharp low-angle reflection and a wide-angle diffuse signal centered at about 4.7 Å (Figure 4). This pattern is characteristic of a disordered layered structure consistent with a smectic phase of A or C type. The above diffraction pattern remains unaffected over the whole range of existence of the mesophase, only a progressive reduction of the layer thickness with increasing temperature is observed. The largest value of the layer spacing in the smectic phase is ≈38 Å, a length considerably smaller than the length of **2d** (l = 51.5 Å) estimated from a model where the aliphatic chains are in their fully extended, all-*trans* conformation (Table 2). Figure 5 shows the temperature dependence of the d spacing corresponding to the dominant reflection, *i.e.*, the maximum periodicity in the solid phase and the layer thickness in the mesophase. A progressive increase is observed up to $T \approx$ 70 °C, where the maximum value of d = 39 Å is reached, followed by an almost linear decrease which finally results in a value of $d \approx$ 35.5 Å at T = 180 °C.

Table 2. Estimated Molecular Lengths l (Å) of Ligands 2 for Various R[a]

n	0	6	10	11	12	14
l	20.0	35.8	46.3	48.9	51.5	56.8

[a] R = p-C_6H_4–O-n-C_nH_{2n+1}; aliphatic chains in their fully extended conformation.

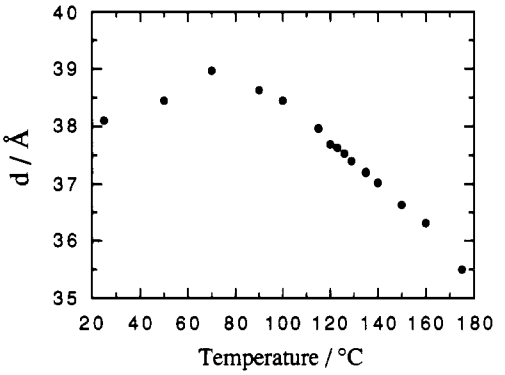

Figure 5. Temperature dependence of the main Bragg periodicity d of [Cu(**2d**)][PF_6].

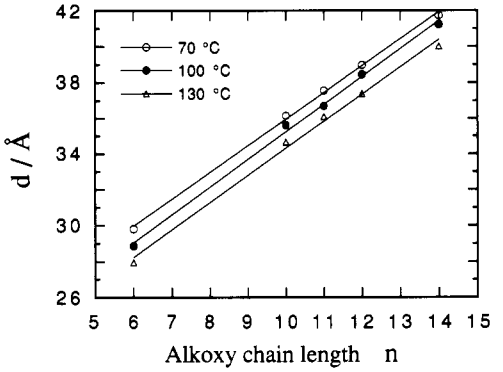

Figure 6. Trend of the d spacing of [Cu(**2a–e**)][PF_6] as a function of the alkoxy chain length at different temperatures. The continuous lines are the linear fit to the experimental data.

The X-ray diffraction measurements performed on the other complexes of the series evidenced for the mesophases the same disordered smectic nature and a similar temperature behavior of the smectic layer spacing. However a remarkable difference between complex [Cu(**2d**)][PF_6] and all the other members of the series was found in the low-temperature solid phase of the pristine sample. In fact, the RT diffraction pattern for those complexes, which displays only one sharp intense low-angle peak and a wide-angle broad diffuse halo, is almost identical to the pattern exhibited in the mesophase. The only modification of the spectrum is a shift of the position of the diffraction peak, with a temperature dependence which follows a trend similar to that observed for [Cu(**2d**)][PF_6]. Figure 6 reports the trend of the d spacing of [Cu(**2a–e**)][PF_6] as a function of the alkoxy chain length n at different temperatures. As it is apparent from the figure, there is a regular increase of the parameter d with increasing n. From the slope of the straight lines fitting the experimental data we always obtain a value of ≈1.5 Å for the projection of two C–C bonds in the polymethylene chain, a value which is only 60% of the projection of two bonds in the all-*trans* conformation. This result suggests either a molecular arrangement where the chains are packed with

(27) Shaffer, T. D.; Sheth, K. A. *Mol. Cryst. Liq. Cryst.* **1989**, *172*, 27.
(28) Versace, C. C.; Bartolino, R.; Ghedini, M.; Neve, F.; Armentano, S.; Petrov, M.; Kirov, N. *Liq. Cryst.* **1990**, *8*, 481.

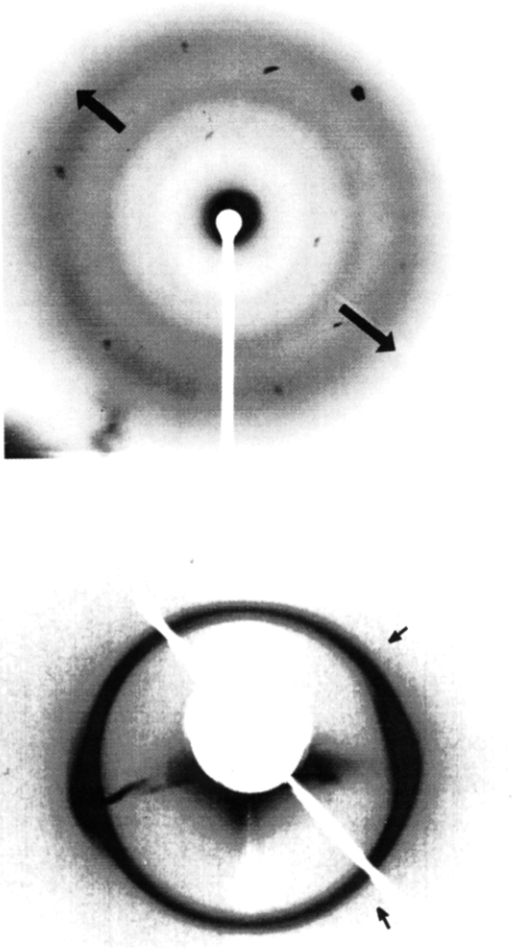

Figure 7. (a, top) Digitalized image of the wide-angle diffraction pattern of an aligned sample of [Cu(**2d**)][PF_6]. The stretching direction is indicated by the arrow; the plane of the mica substrate is perpendicular to the incident beam, giving a few Bragg spots superimposed upon the sample pattern. (b, bottom) Digitalized image of the small-angle diffraction pattern of the same sample. The mica substrate is oscillating around a mean position parallel to the incident beam; the arrows point out the faint 101 reflections.

a considerable tilt angle with respect to the layer normal or a high degree of chain melting. Molecular interdigitation is another possibility.

To clarify the nature of the mesophases and gain a better view of the molecular structural arrangement within the layers, X-ray diffraction measurements on an aligned sample of [Cu(**2d**)][PF_6] have been performed. The mesophase is very viscous and alignment was obtained under shear stress. X-ray experiments have been performed on samples aligned on thin mica crystals and quenched at room temperature, using a point focusing monochromatic Cu Kα beam diffracted by a doubly bent pyrolitic graphite monochromator. The diffraction pattern presents several sharp and diffuse rings (Figure 7). Surprisingly, the innermost ring is sharp and located in a plane perpendicular to the stretching direction, the corresponding lattice spacing being 39.0 Å at room temperature (38.9 Å at 160 °C). The second and third harmonic of this reflection are also seen in the same plane, but they are very weak. The geometry of the X-ray pattern is then that of a columnar mesophase but with evidence of only one-dimensional periodicity. This situation is similar to that of the first patterns obtained with macrocyclic mesogens bearing six aliphatic chains.[24] However, the present macrocyclic molecule presents some differences with respect to the latter mesogens. First, the presence of a copper atom surrounded by four sulfurs at the center of the molecule must increase the structure factor of the mesophase at high angles. Equatorial reflections characteristic of a two-dimensional lattice must likely appear in this case. Secondly, the number and the position of the aliphatic chains give a global rodlike shape to this molecule and the formation of circular columns is unlikely. In fact one other sharp faint diffraction line is located out of the equatorial plane, the corresponding lattice spacing being 33.9 Å. This ring is in fact made of arcs centered on lines perpendicular to the equatorial plane and passing throughout the 001 nodes (39 Å ring). Therefore, these arcs can be assigned as 101 nodes of a rectangular lattice, the main ring located in the equatorial plane being the 001 node. Another ring at 25.6 Å is also seen in some patterns but with much more difficulties. All the sharp rings correspond to the same rectangular lattice: a = 68.2 Å, c = 39.0 Å.

From these data a ribbon structure could be derived, but surprisingly the a axis orients itself in a direction parallel to a shear stress, while the c axis is in the perpendicular plane. This is unusual since generally in columnar phases the columns (or the ribbons) orient themselves parallel to the sheer direction. Another point is the fact that the lattice area (2660 Å^2) is large by comparison to the molecular length and width (51.5 and 5–6 Å, respectively). Taking into account the very weak intensity of the 101 and 102 lines,[29] the periodicity along a seems more likely issued from weak density modulation of a mean layer structure, rather than from the existence of well defined columns. The lattice vectors a and c define the period of modulation and the layer thickness, respectively. The 100 line which should take place on the meridian is not visible, and therefore there is no modulation of the in-plane density, i.e., we have a static undulation of the layers with a period of 68.2 Å. This undulation is similar to the one observed at the transition between smectic B and G phases in some (alkoxy)benzylidene alkylanilines.[30] However, in our system the intralayer ordering is liquidlike (and locally of smectic C type) but the orientation of the layer normal varies periodically around the director.

The undulation corresponds to a local curvature of the layer, the origin of which could be find in a mismatch between the core and chain closest distances. The consequence of a similar mismatch upon the nature of the mesophases have been discussed by Charvolin and Sadoc[31] in the case of amphiphilic films and by De Gennes for columnar phases of disklike molecules.[32] In our case the structure of the layers presents some similarity with the theoretical model of De Gennes; however, there is no core density modulation. Moreover, the modulation in the chain orientation is in phase opposition on the two sides of the medium plane of each layer (Figure 8).

An estimation of the core–core distance can be found in the wide-angle region of the diffraction pattern. Three diffuse rings are seen corresponding to mean distances of

(29) We are not able to assert the existence of the 101 and 102 lines at high temperature.

(30) Leadbetter, A. J.; Mazid, M. A.; Kelley, B. A.; Goodby, J.; Gray, G. W. *Phys. Rev. Lett.* **1979**, *43*, 630.

(31) (a) Sadoc, J. F.; Charvolin, J. *J. Phys.* (*Paris*) **1986**, *47*, 683. (b) Charvolin, J.; Sadoc, J. F. *J. Phys.* (*Paris*) **1987**, *48*, 1559.

(32) De Gennes, P. G. *J. Phys. Lett.* (*Paris*) **1983**, *44*, L657.

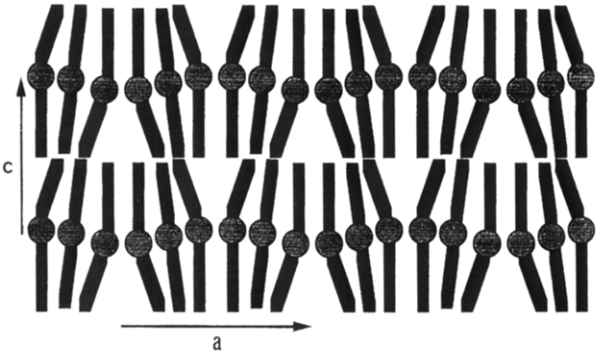

Figure 8. Schematic representation of the undulating layers. An undulation of the molecular cores (including the anions) is correlated to a chain density modulation. The chain modulation is not necessarily to explain the X-ray data but appears naturally as a consequence of the layer curvature. The cores are represented by circles and the chains by bars.

about 8.8, 5.9, and 4.5 Å, the last corresponding to the paraffinic chains in a molten state. The width of the 5.9-Å ring increases with the temperature and at 160 °C the corresponding maximum in intensity looks like a shoulder on the inner side of the main maximum at 4.5 Å. A mean intermolecular distance of 5.9 Å and a mean molecular area of $(5.9)^2$ Å^2 gives a reasonable value for the mesophase density of 0.98 g cm^{-3}. Moreover, the molecular area of 34–35 Å^2 is consistent with typical chain areas in mesophases. The diffuse ring at 8.8 Å is not explained by intermolecular interferences, but it could be explained by intramolecular interferences between the two phenyl rings of the same complex. Finally, considering the ionic nature of the mesophase a contribution to the long-range modulation of the Coulombic interactions is not excluded.

In conclusion it is possible to provide a coherent description of the molecular organisation of the mesophase based upon a monomeric structure of the copper complex cation (structure A). However the interpretation of the X-ray pattern is not at all straightforward and a different chemical structure like a polymeric ribbon (B) giving a sanidic mesophase[33] could not be excluded on the basis of the X-ray data alone.

Conclusions

Saturated macrocyclic ligands with a calamitic molecular shape[34] have been obtained in a straightforward way.

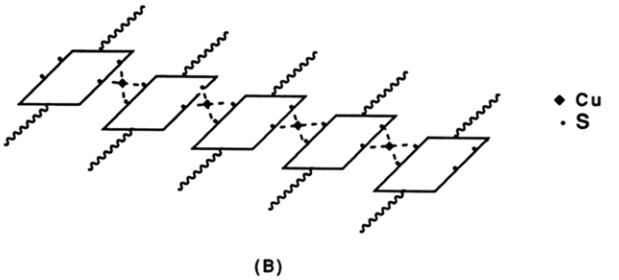

(B)

Mesomorphism was thereupon induced by copper coordination, thus affording the first series of copper(I) metallomesogens.

If one locates the metal ion inside the macrocyclic cavity of **2**, these ionic complexes are similar in shape to the $[Pd(L)][BF_4]_2$ (L = **2a**, **2d**) complexes previously reported.[21] Nevertheless, at least two differences must be considered. On the one hand, the Pd(II) complexes are dicationic species (as opposite to the monocationic Cu(I) species), and on the other, a different coordination geometry is very likely in Cu(I) and Pd(II) complexes (*tetrahedral* vs. *planar*). The above differences are reflected in the different thermal behavior of the complexes. However, the different degree of completeness does not allow a fair comparison of experimental data.

It has been questioned whether mesomorphic complexes incorporating tetrahedral metal centers can be obtained or not. It is said that a tetrahedral geometry does not allow intermolecular ligand–metal dative interactions and this would prevent or strongly disfavor mesomorphism.[1a,c] However, it is well established that intermolecular dative interactions are not necessary in order that mesomorphism takes place. This can be especially true in the case of ionic metallomesogens, since Coulombic attractive forces are primarily responsible for lattice organisation.

Although we cannot exhibit X-ray structural data of single crystals, nevertheless our believe is that the synthesis of this class of Cu(I) mesogens is another step toward an increasing number of coordination geometries compatible with calamitic mesomorphism.

Acknowledgment. Financial support from the Italian Ministero per l'Università e la Ricerca Scientifica e Tecnologica is gratefully acknowledged. We would like to thank Prof. M. Longeri for the 2-D NMR experiment and Prof. G. Sindona for the mass spectra.

(33) Ebert, M.; Herrmann-Schönherr, O.; Wendorff, J. H.; Ringsdorf, H.; Tschirner, P. *Makromol. Chem., Rapid Commun.* **1988**, *9*, 445; *Liq. Cryst.* **1990**, *7*, 63.

(34) It is also possible that **2** assumes a molecular conformation substantially different from a linear one and energy-minimization calculations are needed to clarify this point.